Complex vector fitting toolbox: a software package for the modelling and simulation of general linear and passive baseband systems

Domenico Spina,[1,✉] Yinghao Ye,[3] Dirk Deschrijver,[1] Wim Bogaerts,[2] and Tom Dhaene[1]

[1]IDLab, Department of Information Technology, Ghent University-imec, Gent, Belgium

[2]Photonics Research Group, Department of Information Technology, Ghent University-imec, Gent, Belgium

[3]Faculty of Big Data and Information Engineering, Guizhou University, Guizhou, China

✉Email: domenico.spina@ugent.be

Complex vector fitting (CVF) is a robust method to efficiently and accurately model general linear and passive baseband systems. Such models are important for the analysis and design of modern electronic and optical communication systems. This letter introduces an efficient toolbox implementation of the CVF algorithm. The effectiveness of the code is illustrated on a suitable application example.

Introduction: Due to the increasing demand for performance, the channel bandwidth of modern telecommunication systems is progressively increasing. Examples include 5G networks operating at mmWave or fibre-optic communication links designed in the terahertz bandwidth. The baseband equivalent representation of signals and systems is widely used to simplify the modulation, demodulation and filtering processes typically adopted in communication systems [1]. As such, this representation is well suited to model and simulate digital components, such as finite or infinite impulse response filters. The complex vector fitting (CVF) technique [2, 3] extends the application of the baseband equivalent representation to radio frequency (RF) analog devices, which are fundamental parts of modern communication systems (i.e. microwave filters are typically adopted in front-end circuits), leading to a comprehensive, accurate and efficient modelling framework for baseband systems.

Goal: The aim of this letter is to introduce a CVF toolbox, implemented in MATLAB (Mathworks, Inc., Natick), that facilitates the modelling and simulation of general analog and passive baseband systems. It is available in [4].

Problem formulation: The signals of interest in communication applications are often amplitude and/or phase-modulated signals:

$$y\,(t) = A\,(t)\cos\left(2\pi f_0 t + \varphi\,(t)\right) \qquad (1)$$

where $A(t)$ and $\phi(t)$ are the modulating signals over a carrier with frequency f_0. In particular, the bandwidth of such modulating signals is often significantly smaller than f_0. Signals in the form (1) are also called bandpass signals, and their complex-valued baseband equivalent can be defined as

$$y_b\,(t) = A\,(t)\,e^{j\varphi(t)} \qquad (2)$$

The baseband representation aims at removing the dependency from the carrier frequency in Equation (1), resulting in a spectrum that is defined at significantly lower frequency values, as shown in Figure 1.

A similar operation can be defined for the transfer function $H(f)$ of a linear and passive system [5]: its baseband equivalent is

$$H_b\,(f) = H_+\,(f - f_0) \qquad (3)$$

where $H_+(f)$ represents the spectrum of $H(f)$ defined at positive frequencies, as shown in Figure 2. Note that, if Equation (1) represents a signal at the input port of a bandpass system with transfer function $H(f)$, then Equation (2) is the corresponding port signal of the baseband sys-
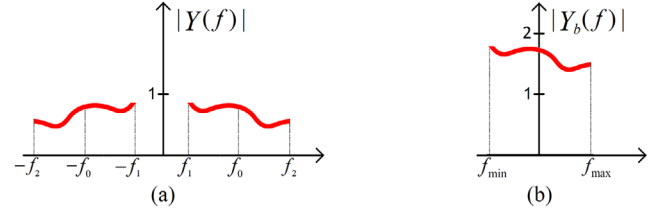

Fig. 1 *Example of (a) bandpass signal spectrum, (b) corresponding baseband equivalent. Note that the baseband spectrum has double magnitude with respect to the corresponding bandpass one [5]*
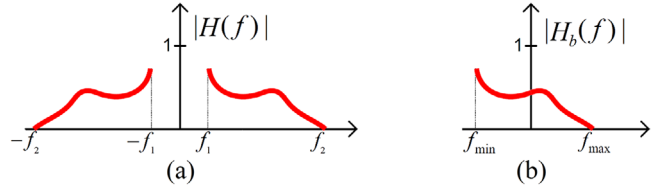

Fig. 2 *Example of (a) magnitude of the transfer function of a bandpass system, (b) corresponding baseband equivalent*

tem defined by $H_b(f)$. Once a suitable model of $H_b(f)$ is computed, time-domain simulations can be performed very efficiently [2, 3], since the bandwidth of baseband signals and systems does not depend on the value of the carrier frequency. Additionally, bandpass port signals can be analytically recovered from their equivalent baseband representation, as shown in Equations (1) and (2).

General, linear and passive baseband systems have an asymmetric frequency response (w.r.t. positive and negative frequencies), leading to a complex-valued impulse response [5]. The CVF algorithm is able to compute an accurate frequency-domain rational model, starting from a set of tabulated baseband scattering parameters $S_b(f_i)$ for $i = 1, \dots, R$

$$\boldsymbol{S}_b\,(s) = \sum_{k=1}^{K} \frac{\boldsymbol{R}_k}{s - p_k} + \boldsymbol{D} \qquad (4)$$

where $s = j2\pi f$ is the Laplace variable; p_k are the poles, which can be either real or complex; $\boldsymbol{R}_k \in \mathbb{C}^{N \times N}$ are the corresponding residue matrices, where N is the number of ports of the baseband system, while $\boldsymbol{D} \in \mathbb{R}^{N \times N}$. For time-domain simulations, models in the form (4) can be suitably converted into a system of ordinary differential equations:

$$\begin{aligned} \frac{d}{dt}\boldsymbol{x}_b\,(t) &= \boldsymbol{A}\boldsymbol{x}_b\,(t) + \boldsymbol{B}\boldsymbol{a}_b\,(t) \\ \boldsymbol{b}_b\,(t) &= \boldsymbol{C}\boldsymbol{x}_b\,(t) + \boldsymbol{D}\boldsymbol{a}_b\,(t) \end{aligned} \qquad (5)$$

where $\boldsymbol{a}_b(t) \in \mathbb{C}^{N \times 1}$ and $\boldsymbol{b}_b(t) \in \mathbb{C}^{N \times 1}$ represent the baseband equivalent of the incident and reflected waves, respectively. The state variables are collected in the vector $\boldsymbol{x}_b(t) \in \mathbb{C}^{M \times 1}$, where $M = NK$ is the order of the model. The matrices $\boldsymbol{A} \in \mathbb{C}^{M \times M}$, $\boldsymbol{B} \in \mathbb{R}^{M \times N}$, $\boldsymbol{C} \in \mathbb{C}^{N \times M}$ and $\boldsymbol{D} \in \mathbb{R}^{N \times N}$ are the baseband state-space matrices and can be computed directly from the pole/residue model in Equation (4) [2, 3].

Note that models in the forms (4) and (5) can be computed for *bandpass* systems adopting the Vector Fitting (VF) algorithm [6–9]. However, VF is not able to model directly baseband systems because it enforces the model to be conjugate symmetric [3].

CVF toolbox: CVF adopts the Sanathanan–Koerner iteration to iteratively compute the model parameters in Equation (4) by successively solving several linear approximations of the non-linear identification problem. This method starts from an initial estimate of the poles in Equation (4), indicated as $p_k^{\text{in}} = \alpha_k + j\beta_k$. The imaginary part β_k is usually chosen as linearly or logarithmically spaced over the frequency range of interest $[2\pi f_{\min};\ 2\pi f_{\max}]$, whereas the real part α_k is set to $\alpha_k = -c|\beta_k|$, with $c = 0.001$. User-defined choices of the starting poles are also supported. The order of the model K can be used to tune the model complexity [10].

The standard VF implementation [6, 7] enforces the model to be conjugate symmetric. This constraint is necessary to ensure that the time-domain impulse response of the system under study is real-valued, which is a fundamental property of physical bandpass systems [5]. However, baseband systems have a complex-valued impulse response by definition. Therefore, the conjugacy constraints in the VF algorithm are removed. Once this fundamental difference is taken into account, several extensions can be integrated into CVF, such as the relaxed formulation [11], which improves the convergence performance, and the fast QR step [7], which speeds up the calculation for multiport systems.

It is important to remark that given the relation among bandpass and baseband transfer functions in Equation (3), bandpass scattering parameters can be easily represented via a baseband CVF model for frequency-domain analyses. In this case, CVF offers a significant advantage: it is able to compute (indicatively) half-size models with respect to VF for the same applications since complex poles and residues do not form conjugate pairs.

Stability and passivity of the model are also crucial for time-domain simulations [5]. Stability can be ensured using a simple pole flipping scheme [6], while passivity needs to be enforced in a post-processing step. In particular, passivity requires that the maximum singular value of the scattering parameters is bound by unity at all frequencies (a detailed derivation of the passivity conditions of baseband systems is presented in [5]). This condition can be verified by checking the eigenvalues of the following Hamiltonian matrix [3]:

$$M = \begin{bmatrix} A - BL^{-1}D^H C & -BL^{-1}B^H \\ -C^H Q^{-1}C & -A^H + C^H DL^{-1}B^H \end{bmatrix} \quad (6)$$

where $L = D^H D - I$, $Q = DD^H - I$, I is the identity matrix, the superscript H indicates the Hermitian operator, while A, B, C, D are the state-space matrices in Equation (5). In particular, a complex-valued and stable state-space model is passive if its Hamiltonian matrix has no purely imaginary eigenvalues. Indeed, each imaginary eigenvalue indicates a crossover frequency where a singular value of the scattering matrix crosses the unity line [5, 12]. If necessary, the passivity can be enforced by perturbing the residue matrix eigenvalues until the violating singular values become smaller than unity.

The CVF toolbox adopts the technique [12] for the passivity assessment and enforcement, suitably adapted to the unique characteristics of baseband systems. Note, however, that half-size passivity tests [13] are no longer applicable due to the presence of the Hermitian operator in Equation (6). Furthermore, both positive and negative frequency values must be considered to individuate the frequency bands where passivity violations occur. Finally, the approach [12] assumes conjugate symmetry, which is not the case for CVF. Hence, equations (22b) and (22c) in [12] become

$$f(s) = \frac{1}{s - p}$$

$$g(s) = \frac{j}{s - p}$$

where p represents a single complex pole in Equation (4).

The proposed CVF implementation is based on the Matrix Fitting Toolbox version 1.0 (available in [14]), which offers a robust implementation of the VF algorithm.

Application example: As an example, the scattering parameters of the coupled microstrips described in [15] and shown in Figure 3 are modelled. The conductors have length $l = 5$ cm and width $w = 120 \, \mu$m. The spacing between the microstrips is $s_1 = 200 \, \mu$m and $s_2 = 100 \, \mu$m. The substrate is a Roger RT/duroid 5880 with relative permittivity $\varepsilon = 2.2$ and thickness $h = 127 \, \mu$m. The scattering parameters of the microstrips are simulated in ADS Momentum (Advanced Design System, Keysight Technologies) in the frequency range [30; 90]GHz for 601 linearly spaced frequency samples. By selecting $f_0 = 57$ GHz, the corresponding baseband scattering parameters are defined in the frequency range [−27; 33]GHz. This choice illustrates the ability of CVF to model baseband transfer functions defined for different positive and negative
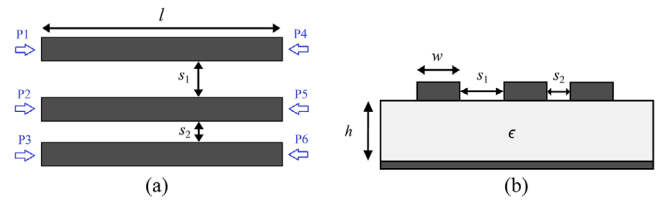

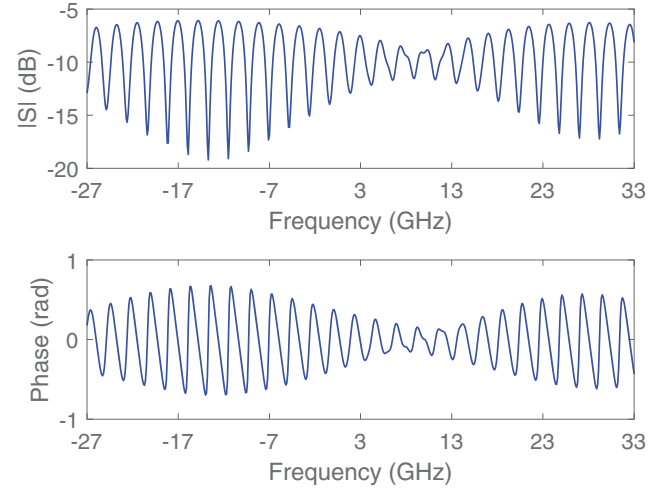Fig. 3 *Coupled microstrips: (a) top view, (b) cross-section*

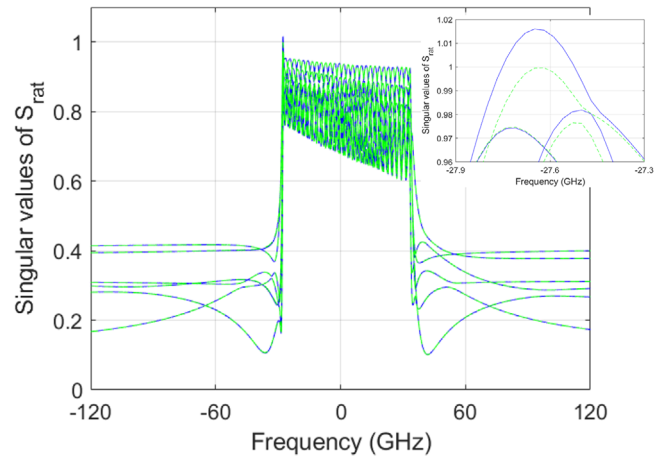Fig. 4 *Element S$_{11}$ of the baseband scattering parameters. Top: magnitude. Bottom: phase*

Fig. 5 *Singular values of the CVF model in the range [− 120; 120]GHz. Blue line: before the passivity enforcement phase. Green dashed line: after the passivity enforcement. The image at the top right corner focuses on the frequencies where the passivity violation occurs before the enforcement step*

frequency values, where $f_{\min} \neq -f_{\max}$ (see Figure 2). The problem under study is quite challenging since the baseband scattering parameters have a dynamic behaviour in the (large) frequency range considered, as illustrated in Figure 4.

The frequency samples are first divided into two groups: modelling points (401 samples) and validation points (201 samples). The first sample set is used to compute the model, while the second one is adopted to verify the fitting accuracy. For this application, a maximum absolute fitting error below − 50 dB is sufficient.

The CVF toolbox is able to compute an accurate and stable rational model with 69 poles, providing also the corresponding state-state representation in Equation (5) to the user. A passivity violation is detected around − 27.5 GHz, which is then corrected using the passivity enforcement process (see Figure 5). Note that the Hamiltonian matrix in Equation (6) of the corrected CVF model does not have purely imaginary eigenvalues, as shown in Figure 6, thus proving the passivity of the corrected CVF model. After the passivity enforcement, the CVF model
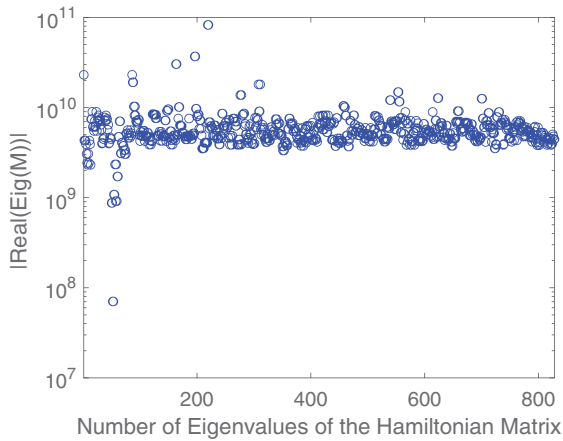
Fig. 6 *Magnitude of the real part of the eigenvalues of the Hamiltonian matrix. All the eigenvalues have real part different than zero*
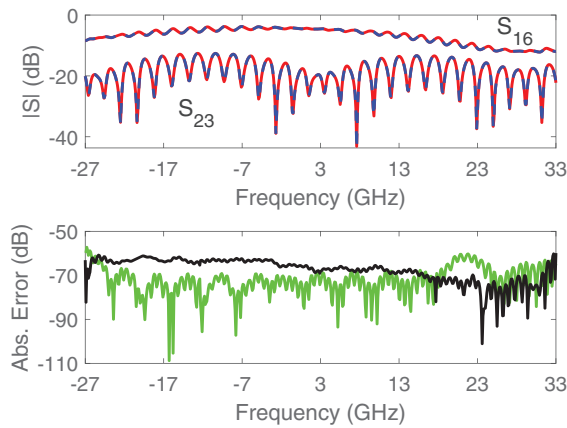

Fig. 7 *CVF modelling results. Top: Comparison of the magnitude of the elements S$_{16}$ and S$_{23}$ of the baseband scattering matrix. The red line indicates the data, while the blue dashed line the CVF model response. Bottom: corresponding absolute error (green for S$_{16}$ and black for S$_{23}$)*
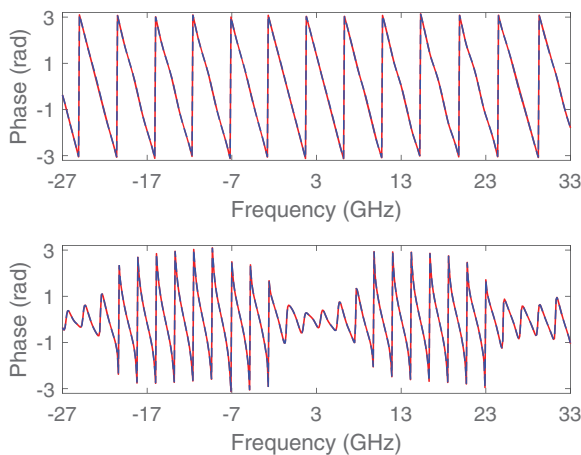

Fig. 8 *CVF modelling results. Top: phase of the element S$_{16}$ of the baseband scattering matrix (red line) and corresponding CVF modelling results (blue dashed line). Bottom: the same comparison is shown for the element S$_{23}$*

still satisfies the chosen accuracy requirements. Figures 7 and 8 show an example of the obtained results: The computed CVF model is able to accurately represent both magnitude and phase of the elements S_{16} and S_{23} of the baseband scattering matrix.

Starting from a set of 69 initial poles, with imaginary part linearly spaced in the frequency range, the model computation required 3.18s and the passivity assessment/enforcement process 5.84s on a computer with an Intel(R) Core(TM) i7-6700HQ CPU and 16GB RAM.

Conclusion: A novel and robust Matlab implementation of the CVF modelling technique is presented in this contribution, capable of computing baseband models of general linear and passive systems. The proposed toolbox allows one to define a comprehensive modelling framework for communication systems, where both digital and analog components can be represented and studied with the baseband equivalent representation.

References

1 Jeruchim, M.C., Balaban, P., Shanmugan, K.S.: *Simulation of Communication Systems: Modeling, Methodology and Techniques*. Springer, Boston, MA (2006)

2 Ye, Y., et al.: Efficient time-domain modeling and simulation of passive bandpass systems. In: International Conference on Electromagnetics in Advanced Applications (ICEAA), Granada, Spain (2019)

3 Ye, Y., et al.: Time-domain compact macromodeling of linear photonic circuits via complex vector fitting. *Photonics Res.* **7**(7), 771–782 (2019)

4 Spina, D., et al.: Complex Vector Fitting toolbox. http://sumo.intec.ugent.be/cvf

5 Ye, Y., et al.: Numerical modeling of a linear photonic system for accurate and efficient time-domain simulations. *Photonics Res.* **6**(6), 560–573 (2018)

6 Gustavsen, B., Semlyen, A.: Rational approximation of frequency domain responses by vector fitting. *IEEE Trans. Power Delivery* **14**, 1052–1061 (1999)

7 Deschrijver, D., et al.: Macromodeling of multiport systems using a fast implementation of the vector fitting method. *IEEE Microwave Wireless Compon. Lett.* **18**(6), 383–385 (2008)

8 Brazil, T. J.: Nonlinear transient simulation of mixed EM/circuit-level system blocks. In: International Conference on Numerical Electromagnetic Modeling and Optimization for RF, Microwave, and Terahertz Applications (NEMO), Pavia, Italy (2014)

9 Grivet-Talocia, S., Gustavsen, B.: Black-box macromodeling and its EMC applications. *IEEE Electromagn. Compat.* **5**(3), 71–78 (2016)

10 Grivet-Talocia, S., Gustavsen, B.: *Passive Macromodeling: Theory and Applications*. Wiley, Hoboken NJ (2016)

11 Gustavsen, B.:Improving the pole relocating properties of vector fitting. *IEEE Trans. Power Delivery* **21**, 1587–1592 (2006)

12 Gustavsen, B.: Fast passivity enforcement for S-parameter models by perturbation of residue matrix eigenvalues. *IEEE Trans. Adv. Packag.* **33**, 257–265 (2010)

13 Gustavsen, B., Semlyen, A.: Fast passivity assessment for S-parameter rational models via a half-size test matrix. *IEEE Trans. Microwave Theory Tech.* **56**, 2701–2708 (2008)

14 Matrix Fitting Toolbox: https://www.sintef.no/projectweb/vectorfitting/downloads/

15 Medico, R., et al.: Machine-learning-based error detection and design optimization in signal integrity applications. *IEEE Trans. Compon. Packag. Manuf. Technol.* **9**(9), 1712–1720 (2019)